

NASA/MODIS PREVIEWS NPOESS/VIIRS CAPABILITIES

Thomas F. Lee
Steven D. Miller
Naval Research Laboratory
Monterey California

Carl Schueler
Raytheon Santa Barbara Remote Sensing
Santa Barbara California

Shawn Miller
Raytheon

Picture of the Month

April 2005

Naval Research Laboratory
7 Grace Hopper Avenue
Monterey California
93943

lee@nrlmry.navy.mil

Abstract

Moderate Resolution Imaging Spectroradiometer (MODIS) true color images offer spectacular renditions of earth and atmospheric phenomena, surpassing the quality and clarity of other satellite images currently available to forecasters from operational satellites. MODIS images can be produced in near real time at Earth Observation Satellite direct readout stations, but relatively few weather forecasters are co-located with such facilities. The majority of other forecasters are hampered by data latency, the time between overpass and image availability, which is typically two to three hours. MODIS is a predecessor to the Visible/Infrared Imager and Radiometer Suite (VIIRS), scheduled to fly on the National Polar-orbiting Operational Environmental Satellite System satellites. Due to a sophisticated downlink and relay system, VIIRS latencies will be 30 min or less (75% of data within 15 minutes) around the globe, improving the timeliness and therefore the operational usefulness of VIIRS images. An image example is shown of coastal stratus in Central California in a comparison to a visible image from the Geostationary Operational Environmental Satellite. In addition, a simulation illustrates improvements in VIIRS scan geometry compared to MODIS.

Multispectral, “true color” images from the Moderate Resolution Imaging Spectroradiometer (MODIS) flying aboard the National Aeronautics and Space Administration’s Earth Observation System (EOS) Terra and Aqua satellites are sharp, colorful and easy for the human analyst to interpret. Given the high spatial and spectral resolution of MODIS, clouds, land, and water features can be seen vividly as in Fig. 1, a summertime scene centered on San Francisco, California. This image was created from the MODIS sensor aboard the Terra (1030 local crossing time) satellite; similar images are available from the Aqua (1330 local crossing time) satellite. Each satellite gives about one regional-coverage image per day over the mid-latitudes, more frequent toward the poles and less frequent toward the tropics. MODIS Terra collects data in thirty-six distinct channels, ranging from $.46\ \mu\text{m}$ in the visible to $14.2\ \mu\text{m}$ in the longwave infrared region. It orbits at an altitude of 705 km with an inclination angle of 98° .

True color images offer a number of qualitative advantages over their panchromatic or false-color counterparts. First, true color is attractive because it simulates what the human eye would see looking down upon the earth from space. Thus, water appears dark blue; vegetation appears green; desert appears in shades of brown; cities often appear gray; and cloud and snow cover appear white. Second, true color images convey a strong sense of realism that facilitates closer inspection by forecasters. The images are not just colorful but allow the observation of fine spatial detail, blending information from the MODIS blue channel ($\sim 0.47\ \mu\text{m}$; 500 m resolution), green channel ($\sim 0.55\ \mu\text{m}$, 500m resolution), and red channel ($\sim 0.65\ \mu\text{m}$; 250 m resolution). For the true color images shown here we interpolate the 500 m channels to 250 m before combining the three channels. STEVE IS THIS SENTENCE CORRECT? REFERENCE?

While true color can be approximated from other satellite data streams lacking these channels, invariably these simulations result in a loss of information or introduction of spurious artifacts. As a result users can often be misled. Geostationary images hold an inherent advantage over polar-orbiting images due to their high temporal refresh, giving important information about the evolution of dynamic systems. However, true color images cannot be produced from present-day geostationary satellites (even the radiometers aboard the next-generation GOES-R series and Meteosat Third Generation satellites will lack this full capability).

The application of true color images to operational environmental monitoring was foreseen by Gumley and King (1995) who used MODIS Aircraft Simulator data to observe floods. The most significant atmospheric research application of true color images to date is probably the imaging of aerosols. Dust, smoke and air pollution tend to disappear on monochromatic satellite images but often appear dramatically in true color and are used to provide context to other scientific results (Chu et al. 2003, Ickoku et al. 2003, King et al. 2003, Koren et al. 2004, and Li et al. 2003,).

For operations, a key limiting factor is timeliness. Users having access to an EOS direct readout station can create such images in real time (for a domain defined by what MODIS can view during line-of-sight contact with the receiver). However, remotely located forecasters typically must wait two to three hours after overpass time to receive the same information, limiting its effectiveness in operational forecasting support. Non-direct-readout latency will improve dramatically to within 30 min when the first National Polar Orbiting Environmental Satellite System (NPOESS) satellite is launched later this decade (Jones 2004). This improvement will be accomplished through a sophisticated

worldwide ground station network, capable of relaying the data to centrals with unprecedented speed.

The GOES 1 km resolution visible images (e.g., top panel of Fig. 1), displayed in near real-time on the Naval Research Laboratory satellite web page (http://www.nrlmry.navy.mil/sat-bin/epac_westcoast.cgi), are accessed routinely by regional forecasters who need little help interpreting them. However, the images are often misinterpreted by less experienced users who depend on these close-up views to make important decisions about agriculture, flood control, fire management, and other issues of public concern. For example, in GOES visible imagery it is difficult based on shades of gray alone to distinguish between forests, agricultural valleys, urbanized zones, and cloud types. Over land, only a few gray tones must account for a broad diversity of surface types. Even offshore, where the ocean background is generally dark and featureless outside of sun glint areas, it is easy to misinterpret the black and white image. What do variations in cloud brightness signify? Satellite meteorologists know how to differentiate between dark areas associated with clear sky regions, thin clouds, and cloud shadows, but untrained users do not.

The true color rendition of the same region (bottom panel of Fig. 1) reveals important additional information. The true color image reveals coastal stratus impinging upon the green forests of the Santa Cruz Mountains, as well as the gray urban detail of the Santa Clara (“Silicon”) Valley in the lee of these mountains (locations in Fig. 2). Further inland, a range of hills known as the East Bay Hills is depicted in shades of brown. In the San Pablo Bay water turbidity effects can be identified based on brown discolorations in contrast to extreme southern end of San Francisco Bay where the water

is less turbid and takes on a deeper blue appearance. Stratus clouds can be seen pouring into San Francisco Bay through the gap spanned by the Golden Gate Bridge. Most of the cloud features appear in the GOES image taken at the same time, but they lack the sharpness and clarity inherent to the 250 m resolution MODIS true color example. Offshore, the white regions correspond to optically thick clouds on the true color image, and varying shades of blue reveal the ocean beneath broken cloud cover. Inexperienced viewers might otherwise mistake these dark areas as cloud shadows if they were only to examine the GOES image.

In the NPOESS era both the timeliness and coverage of true color products will be improved. Through a sophisticated “Safety Net” that consists of a multiple-downlink and fiber optic data relay system, products will be available in fewer than 30 min from overpass time, even for forecasters situated thousands of miles away from the imaged scene (Jones et al. 2004b). At the height of the NPOESS era (a triad of spacecrafts operating simultaneously) there will be three sets of daylight overpasses per 24 h period, supplementing the more frequent geostationary data collection.

NPOESS will host the Visible Infrared Imaging Radiometer System (VIIRS) (Scalione et al. 2004), which will have a swath of about 3000 km vs. 2330 km for MODIS. VIIRS will also be installed on the NPOESS Preparatory Satellite (NPP), a predecessor satellite to NPOESS, scheduled for launch in 2007 (Jones et al. 2004a) with product latencies of about two hours. VIIRS will have 22 channels with a similar channel suite as MODIS. Two spatial resolutions will be employed. “Imager” (I) channels will have a spatial resolution of .38 km at nadir (.371 km downtrack and 0.387 km

crosstrack). “Moderate” (M) channels will have a spatial resolution of .76 km at nadir (.742 km downtrack and 0.776 km crosstrack).

For MODIS (Fig. 3) there is much more pronounced expansion of pixels in the crosstrack than in the downtrack direction. On the other hand, through a procedure described below, crosstrack pixel expansion will be limited for VIIRS (Fig.4) and a nearly square pixel size maintained (Nishihama et al. 1997). Plotting both VIIRS and MODIS functions together (the finest resolution for each) predicts how VIIRS will produce more uniform imagery than MODIS across a scene (Fig. 5). As a result, VIIRS true color images will be less sharp near nadir than MODIS (e.g., Fig. 2) but superior at the edge of swath. The true color input channels on VIIRS are blue (.49 μm ; Moderate resolution); green (.55 μm ; Moderate resolution); and red (.64 μm ; Imager resolution).

The VIIRS accomplishes this improvement of across-track image quality by a unique aggregation method (Schueler 1997), inspired by a similar strategy used by the Defense Meteorological Satellite Program’s Operational Linescan System (DMPS-OLS) (Johnson et al. 1994). For each scan the VIIRS imager will employ a set of “subdetectors” to produce a sequence of “subpixels” each smaller than the nominal pixel size in Fig. 4. The subpixels within this sequence will grow toward the edge of the swath in a similar fashion to MODIS. To produce the functions in Fig. 4, however, the data from adjacent subdetectors will be combined in onboard processing to yield a series of macro pixels at nominal resolution. From about 0 to 32°, three subpixels will be combined to make one nominal pixel. From about 32° to 43°, two subpixels will be combined to make a nominal pixel. Finally, from about 43° to the edge, the subpixels will not be combined, such that the subpixel and the nominal pixel size will be the same.

Within each aggregation regime nominal pixel size grows with scan angle, but the two step functions created by aggregation will reduce overall pixel growth. This strategy will produce higher signal to noise (SNR) near nadir where more aggregation occurs; SNR is lower at the edge of swath where there is no aggregation. However, SNR at the edge still exceeds a priori VIIRS instrument requirements.

For other channels, especially in the middle- and far-infrared, the overall improvement of the spatial resolution of VIIRS compared to MODIS (Table 1) is significantly greater than in Fig. 5, both at nadir and the edge of swath (representative comparison shown in Fig. 6). This improvement follows from the fact that 29 out of 36 MODIS channels are at 1000 m at nadir, comparable to the NOAA Advanced High Resolution Radiometer (AVHRR). In contrast, all 22 VIIRS channels will be at 760 m or better at nadir. Second, pixel expansion is reduced with VIIRS. We simulate this improvement over the northern Persian Gulf (Fig. 7), comparing the 1000 m (nadir) MODIS resolution to a 740 m (nadir) VIIRS resolution based on extremely high-resolution LANDSAT visible data (Fig. 8). We do this by selectively aggregating the LANDSAT data to take the different scan geometries in account. Near nadir the level of detail in MODIS vs. VIIRS is similar; however, the appearance of the MODIS degrades significantly toward the edge. The appearance of the VIIRS image, though minimally degraded, is distinctly sharper.

Table 1 VIIRS Channels

Band Number	VIIRS Wavelength (μm)	VIIRS Nadir Pixel Size (km)	MODIS Nadir Pixel Size (km)	Primary Application
M1	0.41	0.76	0.5	Ocean Color, Aerosols
M2	0.45	0.76	1.0	Ocean Color, Aerosols
M3	0.49	0.76	1.0	Ocean Color, Aerosols
M4	0.55	0.76	1.0	Ocean Color, Aerosols
I1	0.64	0.38	.25	Imagery
M5	0.67	0.76	1.0	Ocean Color, Aerosols
M6	0.75	0.76	1.0	Atmospheric Correction
I2	0.86	0.38	.25	Vegetation
M7	0.86	0.76	1.0	Ocean Color, Aerosols
DayNight	0.7	0.74	N/A	Imagery
M8	1.24	0.76	0.5	Cloud Particle Size
M9	1.38	0.76	1.0	Cirrus Cloud Cover
M10	1.61	0.76	0.5	Binary Snow Map
I3	1.61	0.38	0.5	Snow Cover
M11	2.25	0.76	0.5	Clouds
M12	3.70	0.76	1.0	Sea Surface Temperature (SST)
I4	3.74	0.38	1.0	Imagery, Clouds
M13	4.05	0.76	1.0	SST, Fires
M14	8.55	0.76	1.0	Cloud Top Properties
M15	10.76	0.76	1.0	SST
I5	11.45	0.38	1.0	Cloud Imagery
M16	12.01	0.76	1.0	SST

NRL hosts near real-time true color examples from MODIS similar to the example presented here on its “NexSat” web page, found at http://www.nrlmry.navy.mil/nexsat_pages/nexsat_home.html. Developed under the auspices of the NPOESS Integrated Program Office, NexSat displays products from operational (Johnson et al. 1994) and research polar satellites to anticipate the improvements coming with the next-generation VIIRS system aboard NPOESS. In addition to true color close-ups of over 50 major cities across the continental United States, NexSat features a variety of other products covering regional and national (lower

48 states) scales, including cloud top heights, cloud properties, blowing dust (e.g., Miller 2003), cloud layers, cirrus, cloud over snow cover, contrails, vegetation index, low clouds at night, and nighttime light detection. NASA/MODIS, the National Oceanographic and Atmospheric Administration (NOAA) AVHRR, DMSP-OLS, and GOES East/West imagers all supply NexSat with a comprehensive array near real-time products. With online training modules for each product and an extensive online archive, NexSat appeals to an audience that includes the academic, private sector, government, and general public communities.

Acknowledgements: The data used in this study were acquired as part of the NASA's Earth Science Enterprise through the NASA Goddard Distributed Active Archive Center (DAAC). The support of the research sponsor, the National Polar-orbiting Operational Environmental Satellite System's (NPOESS) Integrated Program Office (IPO) located in Silver Spring, MD, is gratefully acknowledged.

References:

Chu, D.A., Y.J. Kaufman, G. Zibordi, J.D. Chern. J. Mao, C. Li, B.N. Holben, 2003: Global monitoring of air pollution over land from the Earth Observing System-Terra Moderate Resolution Imaging Spectroradiometer (MODIS), *J. Geophys Res*, 108, 4661, doi:10.1029/2002JD003179.

Gumley, Liam E., and Michael D. King, 1995: Remote Sensing of Flooding in the U.S. Upper Midwest during the Summer of 1993. *Bull. Amer. Met. Soc.*, 76, 933–943.

Ichoku, C., L. A. Remer, Y. J. Kaufman, R. Levy, D. A. Chu, D. Tanre, and B. N. Holben, 2003: MODIS observation of aerosols and estimation of aerosol radiative forcing over southern Africa during SAFARI 2000. *J. Geophys. Res.*, 108, 8499, doi:10.1029/2002JD002366.

Johnson, D.B., P. Flament, and R.L. Bernstein, 1994: High Resolution Satellite Imagery for Mesoscale Meteorological Studies, *Bull. Amer. Met. Soc.*, 75, 5-33.

Jones, D., 2004: The Future of Earth—Sensing from Space, The Next Generation Satellite Series: A Look at NPOESS and Its Benefits. *Earth Observation Magazine*, 13, 1, 4-10.

Jones, D., S.R. Schneider, P. Wilczynski, C. Nelson, 2004a: NPOESS Preparatory Project: The Bridge between Research and Operations. *Earth Observation Magazine*, 13, 3, 12-17; 20-22.

Jones, D., C. Nelson, and M. Bonadonna, 2004b: NPOESS: 21st Century Space-Based Military Support, *Earth Observation Magazine*, 13, 4, 24-30.

King, M.D., S. Platnick, C.C. Moeller, H.E. Revercomb, and D. Allen Chu, 2003: Remote sensing of smoke, land, and clouds from the NASA ER-2 during SAFARI 2000. *J. Geophys. Res.*, 108, 8502, doi:10.1029/2002JD003207.

Koren, I., Y. J. Kaufman, L. A. Remer, and J. V. Martins, 2004: Measurement of the Effect of Amazon Smoke on Inhibition of Cloud Formation. *Science*, 303, 1342-1345.

Li, L., H. Fukushima, R. Frouin, B.G. Mitchell, M.X. He, I. Uno, T. Takamura, S. Ohta, 2003: Influence of submicron absorptive aerosol on sea-viewing wide field-of-view sensor (SeaWiFS)-derived marine reflectance during Aerosol Characterization Experiment (ACE)-Asia. *J. Geophys. Res.*, 108, 4472, doi:10.1029/2002JD002776.

Miller, S. D., 2003: A consolidated technique for enhancing desert dust storms with MODIS, *Geophys. Res. Lett.*, 30, 2071, doi:10.1029/2003GL018279.

Nishihama, M., R. Wolfe, and D. Solomon, cited 1997: MODIS Level 1A Earth Location: Algorithm Theoretical Basis Document Version 3.0. [Available online at modis.gsfc.nasa.gov/data/atbd/atbd_mod28_v3.pdf .].

Scalione, T., H. W. Swenson, F. De Luccia, C. Schueler, J. E. Clement, L. Darnton, 2004:
Post-CDR NPOESS VIIRS sensor design and performance, Proceedings of the SPIE,
Barcelona Spain, 5234, 144-155.

Schueler, C. F., 1997: Dual-use Sensor Design for Enhanced Spatiometric
Performance. US patent No. 5,682,034.

Figure Captions:

Fig. 1 Top: GOES-West visible image for 29 July 2004, 1845 UTC. Yellow contour represents 200 m terrain elevation level. Bottom: Terra true color image for 29 July 2004, 1855 UTC. Image is of central California, where stratus covers the offshore waters to the west and extends inland in the San Francisco Bay region. Coastlines are drawn in orange.

Fig. 2 Study area for Fig. 1. Dimensions are approximately 130 km east/west and 200 km north/south.

Fig. 3 MODIS cross scan variation in pixel size as a function of scan angle away from nadir. Half and quarter km data are used in construction of true color images.

Fig. 4 VIIRS cross scan variation in pixel size as a function of scan angle away from nadir. Both resolutions will be used in the construction of true color.

Fig. 5 Comparison of high resolution “red” input channels required for true color: VIIRS 370 m (nadir) resolution vs. MODIS 250 m (nadir) resolution.

Fig. 6 Comparison of 1000 m (nadir) resolution used for 29 of 36 MODIS channels with 740 m (nadir) resolution for VIIRS. 17 of 22 VIIRS channels use the resolution shown here. Five use a higher resolution of 370 m (nadir). These resolutions are used in the simulations in Fig. 8.

Fig. 7 Map of Southwest Asia. Box contains northern Persian Gulf imaged in Fig. 8.

Fig. 8 Simulation (based on aggregated Landsat data over Iraq) showing MODIS 1 km nadir resolution vs. VIIRS 740m nadir resolution images at nadir and edge of swath (EOS, 53° in Figure 6).

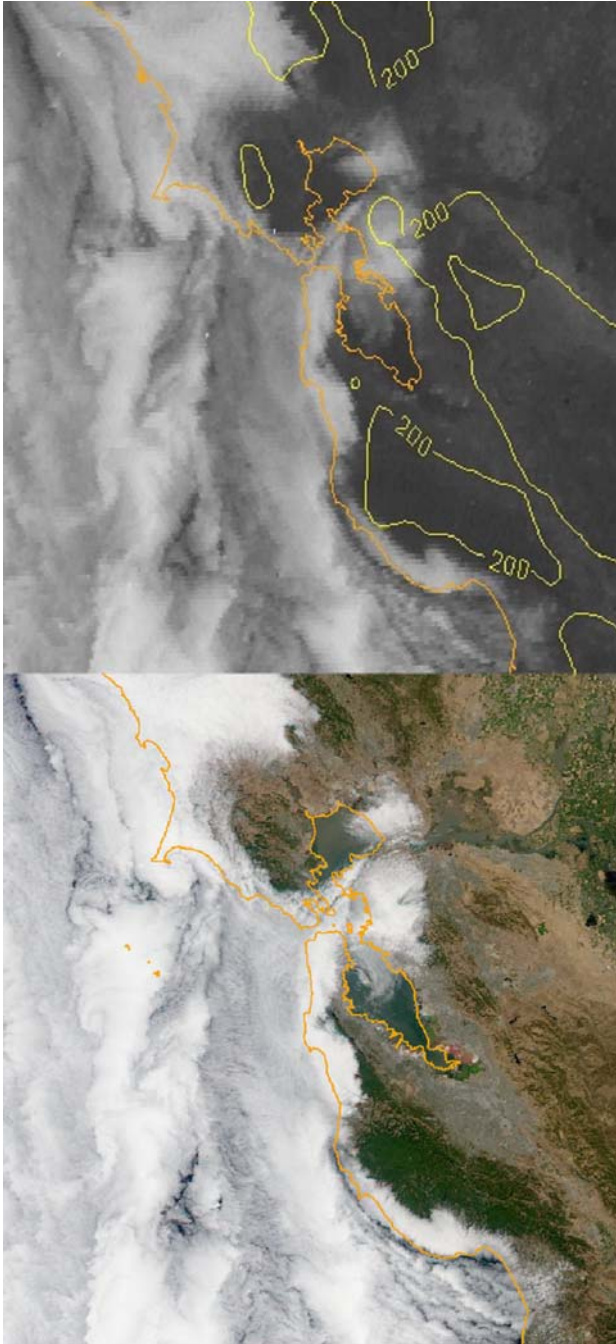


Fig. 1 Top: GOES-West visible image for 29 July 2004, 1845 UTC. Yellow contour represents 200 m terrain elevation level. Bottom: Terra true color image for 29 July

2004, 1855 UTC. Image is of central California, where stratus covers the offshore waters to the west and extends inland in the San Francisco Bay region. Coastlines are drawn in orange.

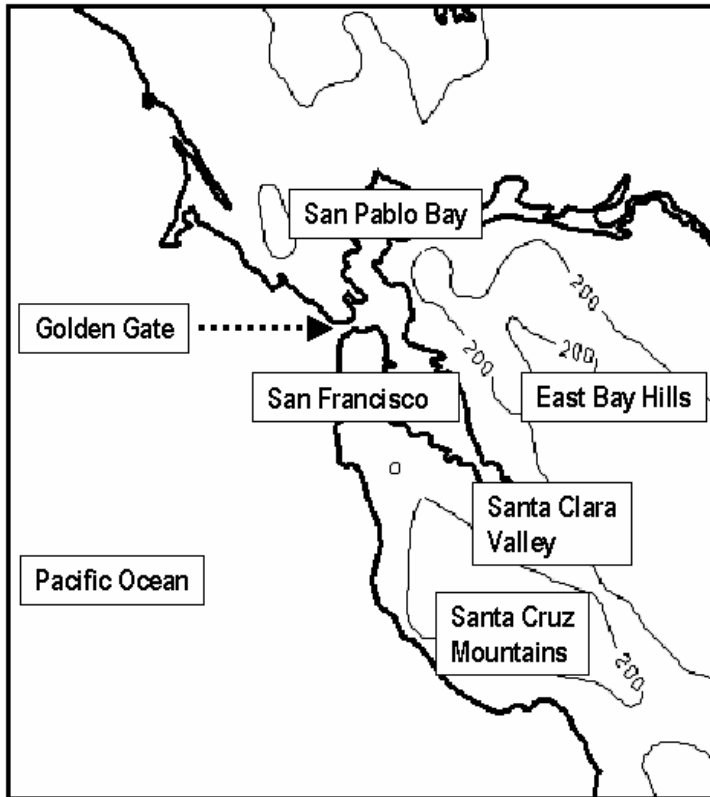


Fig. 2 Study area for Fig. 1. Dimensions are approximately 130 km east/west and 200 km north/south.

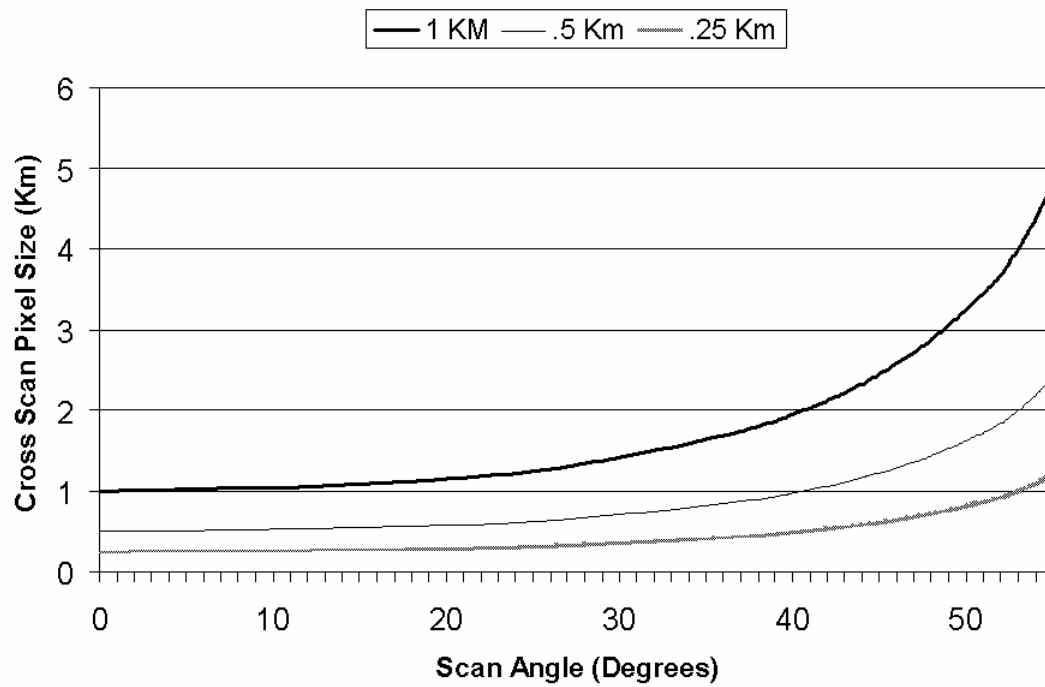


Fig. 3 MODIS cross scan variation in pixel size as a function of scan angle away from nadir. Half and quarter km data are used in construction of true color images.

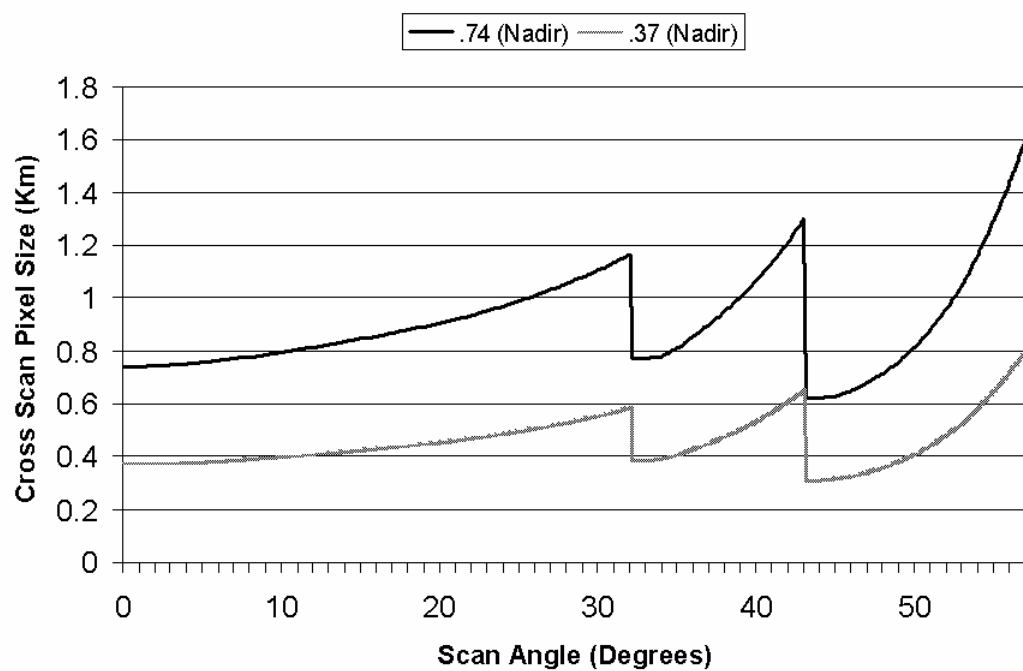


Fig. 4 VIIRS cross scan variation in pixel size as a function of scan angle away from nadir. Both resolutions will be used in the construction of true color.

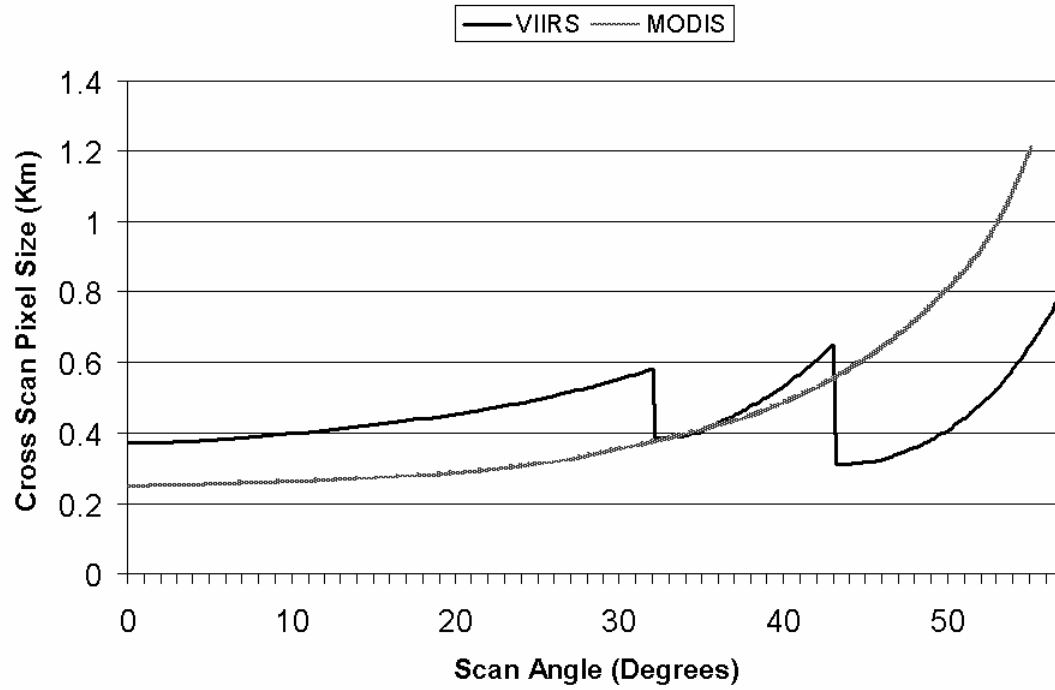


Fig. 5 Comparison of cross scan pixel size for high resolution “red” input channels required for true color: VIIRS 370 m (nadir) resolution vs. MODIS 250 m (nadir) resolution.

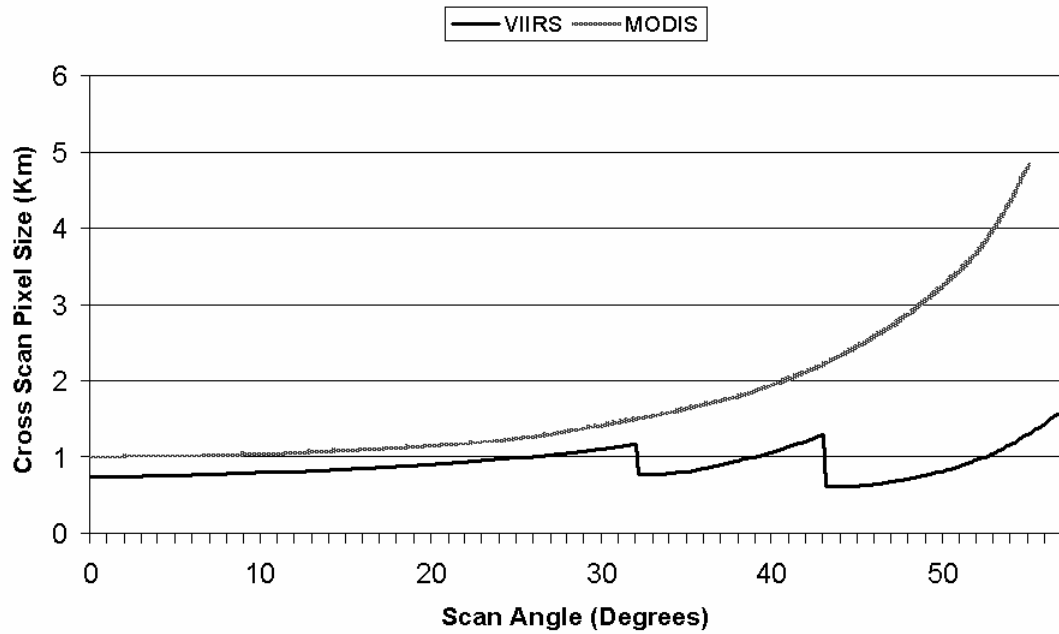


Fig. 6 Comparison of 1000 m (nadir) resolution used for 29 of 36 MODIS channels with 740 m (nadir) resolution for VIIRS. 17 of 22 VIIRS channels use the resolution shown here. Five use a higher resolution of 370 m (nadir). These resolutions are used in the simulations in Fig. 8.

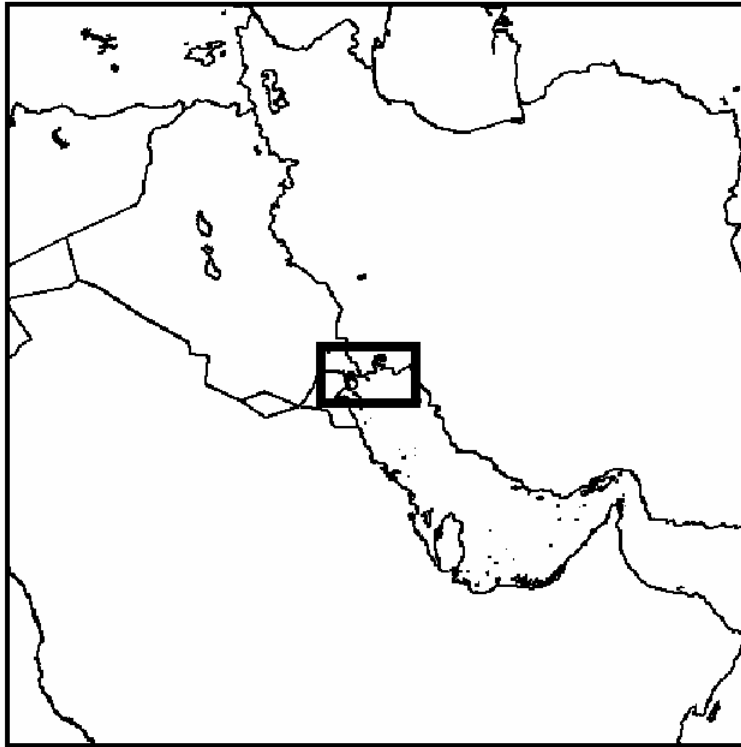


Fig. 7 Map of Southwest Asia. Box contains northern Persian Gulf imaged in Fig. 8.

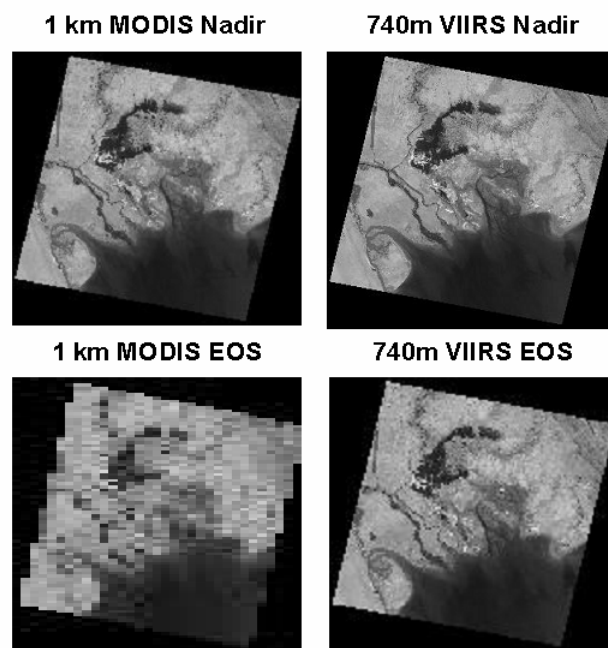


Fig. 8 Simulation (based on aggregated Landsat data over Iraq) showing MODIS 1 km nadir resolution vs. VIIRS 740m nadir resolution images at nadir and edge of swath (EOS, 53° in Figure 6).